

RESEARCH ARTICLE

Metabolomic Characterizations of Liver Injury Caused by Acute Arsenic Toxicity in Zebrafish

Caixia Li¹, Ping Li¹, Yee Min Tan³, Siew Hong Lam^{1,2}, Eric C. Y. Chan³, Zhiyuan Gong^{1,2*}

1 Department of Biological Sciences, National University of Singapore, Singapore, Singapore, **2** NUS Environmental Research Institute, National University of Singapore, Singapore, Singapore, **3** Department of Pharmacy, National University of Singapore, Singapore, Singapore

* dbsgzy@nus.edu.sg



OPEN ACCESS

Citation: Li C, Li P, Tan YM, Lam SH, Chan ECY, Gong Z (2016) Metabolomic Characterizations of Liver Injury Caused by Acute Arsenic Toxicity in Zebrafish. PLoS ONE 11(3): e0151225. doi:10.1371/journal.pone.0151225

Editor: Zhan Yin, Chinese Academy of Sciences, CHINA

Received: October 19, 2015

Accepted: February 23, 2016

Published: March 11, 2016

Copyright: © 2016 Li et al. This is an open access article distributed under the terms of the [Creative Commons Attribution License](https://creativecommons.org/licenses/by/4.0/), which permits unrestricted use, distribution, and reproduction in any medium, provided the original author and source are credited.

Data Availability Statement: All relevant data are within the paper and its Supporting Information files.

Funding: This work was supported by the Singapore National Research Foundation under its Environmental & Water Technologies Strategic Research Programme and administered by the Environment & Water Industry Programme Office (EWI) of the PUB, grant number R-154-000-328-272. The funders had no role in study design, data collection and analysis, decision to publish, or preparation of the manuscript.

Abstract

Arsenic is one of the most common metalloid contaminants in groundwater and it has both acute and chronic toxicity affecting multiple organs. Details of the mechanism of arsenic toxicity are still lacking and profile studies at metabolic level are very limited. Using gas chromatography coupled with mass spectroscopy (GC/MS), we first generated metabolomic profiles from the livers of arsenic-treated zebrafish and identified 34 significantly altered metabolite peaks as potential markers, including four prominent ones: cholic acid, glycyglycine, glycine and hypotaurine. Combined results from GC/MS, histological examination and pathway analyses suggested a series of alterations, including apoptosis, glycogenolysis, changes in amino acid metabolism and fatty acid composition, accumulation of bile acids and fats, and disturbance in glycolysis related energy metabolism. The alterations in glycolysis partially resemble Warburg effect commonly observed in many cancer cells. However, cellular damages were not reflected in two conventional liver function tests performed, Bilirubin assay and alanine aminotransferase (ALT) assay, probably because the short arsenate exposure was insufficient to induce detectable damage. This study demonstrated that metabolic changes could reflect mild liver impairments induced by arsenic exposure, which underscored their potential in reporting early liver injury.

Introduction

Arsenic is one of the most common metalloid toxicants contaminating groundwater and this contamination is a global concern. Two inorganic forms of arsenic, trivalent (As^{3+}) and pentavalent (As^{5+}), are the main forms in groundwater, with As^{5+} as the predominant form in oxidizing conditions [1]. Inorganic arsenic is both acutely and chronically toxic and it is classified as a carcinogen by the International Agency for Research on Cancer [2]. Long-term exposure to arsenic is associated with increased risk of cancers in liver, skin, lungs, bladder and kidney. It can also disrupt the cardiovascular, reproduction, nervous system and immune system [3–5]. 10 µg/L has been set by World Health Organization as the maximal level for arsenic

Competing Interests: The authors have declared that no competing interests exist.

contaminant in drinking water, but millions of people worldwide, particularly in some Asian countries, are still exposed to toxic levels (>50 $\mu\text{g/L}$) due to surface water and groundwater contamination [1]. Molecular mechanisms of arsenic toxicity have been long studied. The involvement of oxidative stress, genotoxicity, altered DNA methylation and others have been reported; however, details of the mechanism of action through an integrated approach are still lacking [6].

Applications of omic approaches in aquatic toxicology have been rapidly increasing as a result of technological development and availability of genome sequences for common aquatic model organisms (e.g. zebrafish, medaka, fathead minnow, and water flea). For arsenic exposure in human, there have been many publications on transcriptome but only a few studies have been conducted on proteome [7] and one on metabolome (mixed exposure to arsenic, cadmium and lead) [8]. Similarly in non-human studies, metabolomic studies on arsenic toxicity are scarce; so far only four reports are on rodents [9–12] and two reports on non-rodents, clam [13] and *Daphnia* [14]. Despite the importance of fish models in aquatic toxicology, arsenic-induced metabolomic changes in fish have not yet been reported.

Among the fish models, the zebrafish (*Danio rerio*) has a unique combination of advantageous traits for scientific research. It has evolutionarily conserved genes and molecular pathways when compared to higher vertebrates, well developed genetic manipulation tools and a large body of literature data, including the complete genome sequences to facilitate genome-wide studies [15]. Studies of arsenic using the zebrafish embryos have reported substantial toxicity during embryogenesis [16], neural defects [17], vascular development [18], immune response [19, 20]. Fewer studies have been performed on adult zebrafish, which usually reported molecular events such as cellular transport of arsenic [21], transcriptomic changes and biomarker gene selection [22], and changes of molecules or pathways of interest [23]. Previously, we have used adult zebrafish to investigate arsenic-induced transcriptomic changes in the liver, the primary detoxification site and target organ of arsenic [3, 24]. In this study, we aimed to assess the changes in liver metabolic profile after 96-hr acute exposure to inorganic arsenic (As^{5+}) using gas chromatography coupled with mass spectroscopy (GC/MS). We identified 34 significantly altered metabolite peaks as potential marker. Liver damages implied by the metabolomic changes were further validated by histological examination but not reflected in two conventional liver function tests. Our study indicated that metabolic markers may be of great potential in reporting early liver damages.

Material and Methods

Acute arsenic exposure in adult zebrafish

The use of zebrafish in this study was in strict accordance with the recommendations in the Guide for the Care and Use of Laboratory Animals of the National Institutes of Health. The protocol was approved by the Institutional Animal Care and Use Committee (IACUC) of the National University of Singapore (Protocol Number: 096/12). Adult male zebrafish of Singapore wildtype strain, aged 6–10 months, were purchased from Mainland Tropical Fish Farm, Singapore and acclimatized for two weeks. Standard 96-hr acute exposures to sodium arsenate ($\text{Na}_2\text{HAsO}_4 \cdot 7\text{H}_2\text{O}$, Sigma) at 20 ppm (for metabolomic profiling) or at 15 ppm (for validation of robust changes at slightly lower concentration) were conducted in replicate tanks of 15 fish each. The control groups were similarly set up without arsenate. Media were renewed once on day 3 of exposure experiment. The water condition and health status of fish were monitored daily. Fish with signs of unrelieved sickness (e.g. inactive, reduced breathing, and staying at only bottom of tank or surface of water) were euthanized with 250 mg/L MS222. At the end of treatment, fish were euthanized in ice water instead of anesthesia to minimized potential

undesirable changes induced on liver metabolome. For metabolic profiling, liver samples were collected as a pool of four livers per replicate and five replicates per group, snap-frozen in liquid nitrogen, and then stored at -80°C until metabolite extraction. Sampling for histological examination and liver function tests are described in separate sections.

Metabolite sample preparation

Metabolite samples were prepared following an established protocol [25] with optimization to maximize extraction from liver. Briefly, 20 mg tissues were homogenized in water (1:10 w/v) using pulse sonication. After a brief centrifugation at 4°C , 100 μL of supernatant was transferred to 1 mL of extraction buffer, a solvent mixture of chloroform-methanol-water (2:5:2 v/v/v) with 0.5 mg/L diclofenac as internal standard, for metabolite extraction in a large capacity mixer for 30 min and centrifuged at 10,000 g at 4°C for 10 min. 800 μL supernatant was aspirated into a salinized glass tube and dried in TurboVap LV nitrogen evaporator (Caliper Life Science) at 50°C for 1 hr. To further dehydrate the extract, 100 μL of toluene (dried over Na_2SO_4) was added, vortex-mixed for 1 min and dried in TurboVap. Metabolites were reconstituted in 40 μL methoxyamine hydrochloride (MOX) for methoxymation at 60°C for 2 hr. For silylation, 60 μL N-Methyl-N-(trimethylsilyl) trifluoroacetamide (MSTFA; Alpha Analytical) was added and incubated at 70°C for 30 min. Processed samples were then transferred to GC vials for GC/MS analysis. For quality assessment of procedures, after pulse sonication in water, 80 μL aliquot from each control replicate was taken and well mixed, from which three 100- μL aliquots were used as quality control (QC) samples, which were then processed in exactly the same way as other samples throughout the experiment.

GC/MS metabolic profiling

GC/MS was performed using a Pegasus 4D TOFMS (LecoCorp) equipped with an Agilent 7890 GC and a CTC CombiPAL autosampler. A DB-1 capillary column (30 m \times 250 μm (i.d.) \times 0.25 μm) with DuraGuard (Agilent Technologies J&W) was used. Helium flow rate was set at 1.5 mL/min and the injection volume was 1 μL with injector split ratio 1:20. For GC, the temperature was 220°C for front inlet and 280°C for transfer line. Column temperature was programmed to be at 70°C for 0.2 min, ramped at $15^{\circ}\text{C}/\text{min}$ to 270°C and then at $40^{\circ}\text{C}/\text{min}$ to 310°C , and finally hold at 310°C for 8 min. For MS, the detector voltage was 1,600 V with an acquisition delay of 200 seconds. To facilitate metabolite identification, alkane standard mix (C10-C40; Sigma) and FAME (fatty acid methyl esters) standards (C8-C28; Sigma) were analyzed using the same settings, so that the GC retention time could be converted to two types of retention index (RI), Kovats index and Fiehn index, respectively.

Data processing

The GC/MS spectra were processed with LECO's ChromaTOF software for peak picking (S/N = 100, peakwidth modulation 2.5 s), tentative metabolite identification by MS spectra matching with library compounds (similarity score > 600), peak alignment, and calculation of RIs. All de-convoluted chromatographs were manually inspected for consistent peak area integration. Missing values were filled by integration of baseline in chromatograph. Peak areas were normalized using quantile normalization (QN), where metabolites were ranked and individual values were substituted with reference to the same ranks in other samples following defined steps. It is expected to make distributions identical in statistical properties [26]. Normalized peaks were cleaned by discarding peaks with coefficient of variance (CV) > 0.3 in QC replicates [25] before chemometric analysis.

Chemometric analysis

Peaks ($CV < 0.3$) were subjected to Principle Component Analysis (PCA), Partial Least Square-Discriminant Analysis (PLS-DA) modeling in SIMCA-P software (version 11, Umetrics) in addition to Welch's *t*-test. PLS-DA model was validated by 1,000 rounds of built-in permutation test. Metabolites with variable importance plot values (VIPs) greater than 1.0 in PLS-DA model was considered to be positively contributing to the group separation. Peaks with $VIP > 1$ and $p < 0.05$ in *t*-test were considered as potential markers.

Identification of metabolites and biological interpretation

Tentative identities of metabolites were obtained by spectra matching as above described. For peaks with $VIP > 1$, spectra hits were inspected and identity of the corresponding underivatized structures were confirmed using ChemSpider (<http://www.chemspider.com/>). RIs were compared to those in the following databases: NIST Chemistry WebBook (<http://webbook.nist.gov/chemistry/>), Human Metabolite Database (HMDB, <http://www.hmdb.ca/>), Golm metabolome database (<http://gmd.mpimp-golm.mpg.de/>) and Metabolomics Workbench (<http://www.metabolomicsworkbench.org/>). Identification status of a metabolite was considered "confirmed" when: (1) its spectrum was highly similar to an item in a library; and (2) both RIs were consistent with literature values. Identification status was considered "probable" when (1) its spectrum was highly similar to an item in library; (2) only one RI was available in literature and the calculated RI was consistent with it. Other metabolites were denoted as "unknown". Metabolites with "confirmed" and "probable" identities were input into Ingenuity Pathway Analysis (IPA) for biological interpretation.

Histological examination

Fish were euthanized by ice and fixed in either 10% formalin (for paraffin section; Sigma) or 4% PFA (for cryosection; Sigma). For paraffin section, fixed samples were gradually dehydrated in ethanol, exchanged into HistoClear (National Diagnostcs), and embedded into paraffin (Sigma). 5 μ m sagittal sections of livers were taken for Hematoxylin & Eosin (H&E) staining, Periodic acid-Schiff (PAS) staining and Tunnel assay. For cryosection, fixed samples were embedded in 1.5% bactoagar containing 5% sucrose and mounted to a cryostat microtome holder in tissue-freezing medium. 8 μ m sections were used for Oil Red O (ORO) staining.

Paraffin sections were de-paraffinized in HistoClear and rehydrated to water before staining. For H&E staining, sections were stained in Mayer's Hematoxylin (Sigma), gradually dehydrated to 90% alcohol, and counterstained in Eosin (Sigma). For PAS staining, sections were oxidized in 0.5% periodic acid (Sigma), incubated in Schiff's reagent (Sigma), and washed in lukewarm water before counterstaining in Mayer's hematoxylin. Tunnel assay was performed using In situ Cell Death Detection Kit, Fluorescein (Roche) according to manufacturer's protocol. For ORO staining, cryosection slides were incubated in absolute propylene glycol (Sigma), stained in 0.5% ORO (Sigma) at 60°C, rinsed in 85% propylene glycol and then in water, and finally briefly counterstained in Mayer's Hematoxylin.

Liver function tests

Bilirubin assay kit and alanine aminotransferase (ALT) activity assay kit (Sigma) were used to assess functional status of fish liver. For bilirubin assay, only plasma was used. For ALT activity assay, both plasma and liver protein extracts were used.

Whole blood was collected at the dorsal aorta after tail ablation using P20 micropipettor fitted to an elongated tip (Prot/Elec Tips, Bio-Rad) and aspirated into pre-chilled Eppendorf tubes.

Both pipette tips and tubes were pre-coated with EDTA (submerging in 18 mg/mL EDTA solution for one day and then dried). Blood of 3–6 fish were pooled as one sample. Plasma was obtained as clear supernatant after centrifugation at 1000 g for 10 min at 4°C and stored at -80°C. Bilirubin assay was completed within 2 days of plasma collection.

To extract total protein, liver tissue was homogenized in ALT assay buffer (1:15 w/v) on ice and then centrifuged at 14,000 rpm at 4°C for 10 min. Supernatant was collected. Protein concentration was estimated based on Bradford method using Bio-Rad Protein Assay Dye Reagent and Bovine Serum Albumin standard (Sigma). ALT assay was performed following manufacturer's protocol, while bilirubin assay was scaled down after confirming the linearity of bilirubin standard ([S1 Fig](#)).

Results and Discussion

Both As^{3+} and As^{5+} are present in environmental water and of concern [1]. In this study, we selected As^{5+} for metabolomic studies because of availability of transcriptomic data we previously generated on As^{5+} exposed zebrafish livers [3, 24] for integrated studies. Fish exposed to 20 ppm and 15 ppm were more lethargic than those in control groups. Survival by the end of exposure was ~80% (25/30) at 20 ppm and 100% (30/30) at 15 ppm. Arsenic is known to be easily absorbed in gastrointestinal tract and biotransformed in liver before distribution to various other organs [27]. The liver is the main organ for bioaccumulation of arsenic in fish and the bioconcentration factors are between 3–13 fold [21, 28–30]. Metabolic profiles of livers from male adult zebrafish in both control and 20 ppm arsenic (As^{5+})-treated group were obtained using GC/MS, in which 331 metabolite peaks were confidently detected. The peak areas (representing abundance of the metabolites) were quantile-normalized and 239 reliable peaks ($\text{CV} < 0.3$ within QC samples) were used for chemometric analysis.

Arsenate treatment changed liver metabolic profile

The 239 peaks were input to SIMCA-P software for PCA and PLS-DA modeling. In PCA plot, three QC samples were clustered tightly among themselves (and with two control replicates), suggesting good quality of sample processing and reproducibility of GC/MS ([Fig 1A](#)); however, the spread of replicates in both control and As groups indicated high biological variations. By PLS-DA modeling, a decent separation of the two groups, largely based on the first component, was observed ([Fig 1B](#)). There were 110 metabolites with $\text{VIP} > 1$, 48 increased and 62 decreased in the As group. From these metabolites, 57 unique metabolites were identified, 25 of which were with status as “confirmed” and 32 as “probable” ([S1 Table](#)). It should be pointed out that, the distance between control and As groups in modeling was small, implying that exposure to 20 ppm As^{5+} caused significant but not extensive changes to the profiles.

To identify potential markers, Welch's t-test was applied to the 110 peaks and 34 of them had $p < 0.05$ ([Table 1](#)). Hierarchical clustering of these 34 potential markers ([Fig 1C](#)) revealed similar patterns among the As replicates. Patterns of control replicates were more variable and one replicate (H2O1) was closer to the As cluster than to the control cluster, which was consistent with the PCA plot. Yet, with a closer examination, the two groups could be distinguished even with only seven selected potential markers ([S2 Fig](#)). 20 out of the 34 potential markers were identified (confirmed or probable), among which cholic acid ($\text{FC} = 1.51$, $p = 0.002$) and glycyglycine ($\text{FC} = 0.57$, $p = 0.0002$) showed best distinction between the two groups in the clustering. Other notable markers were hypotaurine (decreased), four decreased unsaturated lipids (linoleic acid, alpha-linolenic acid, palmitoleic acid, and oleic acid), three decreased amino acids (threonine, glycine and 2-aminobutanoate), and two increased bile acids (urso-deoxycholic acid and chenodeoxycholic acid). Glycyglycine (diglycine) is the simplest

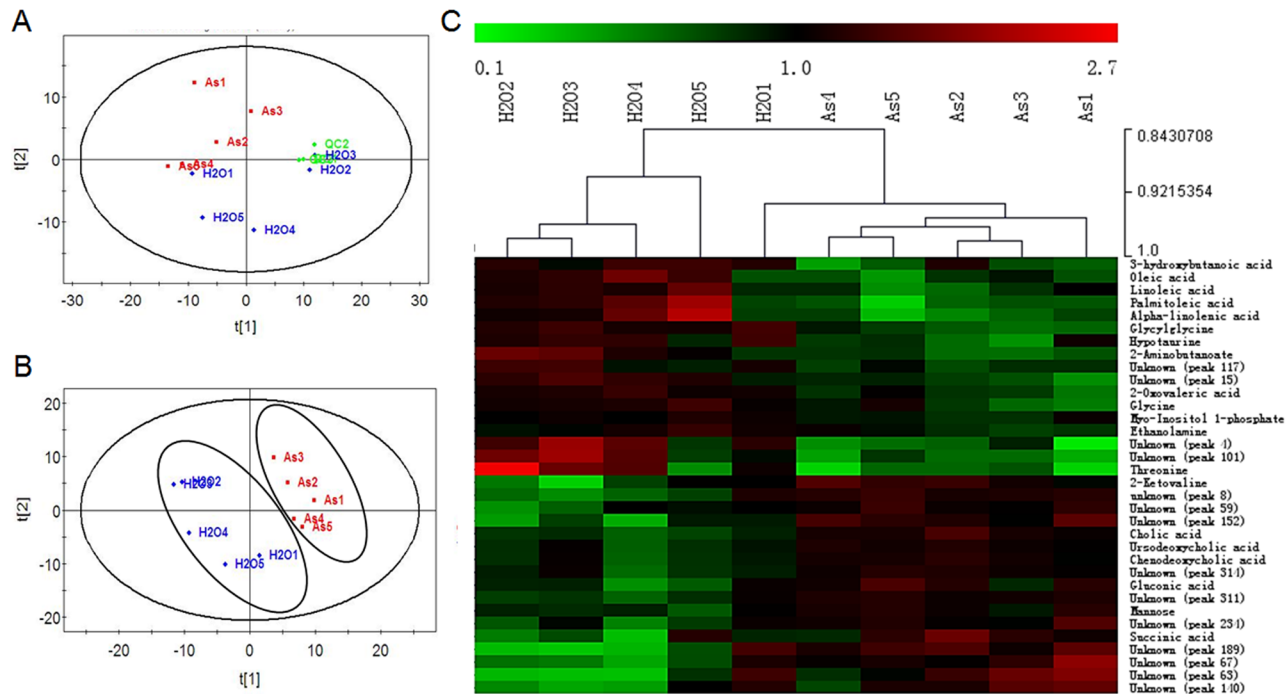


Fig 1. Results of chemometric analysis and hierarchical clustering. (A) PCA plot showing tight clustering of QC samples and inherent separation between control and treated groups. (B) PLS-DA plot with decent separation of the two groups. (C) Hierarchical clustering of samples using peak areas of the 34 potential metabolite markers. Peak areas were quantile-normalized and standardized to respective mean value of each metabolite among all samples. Hierarchical clustering was performed using Pearson correlation method without mean centering.

doi:10.1371/journal.pone.0151225.g001

dipeptide, whose source can be endogenous or exogenous. Hypotaurine is an intermediate in the synthesis of taurine from cysteine. In liver, bile acids need to be conjugated with taurine or glycine to form bile salts for secretion. The concurrent decrease of hypotaurine and glycine may contribute to the accumulation of bile acids. These effects of arsenic on bile acids and hypotaurine in the liver have not been reported before. For glycine, a recently study reported reduction of glycine in mouse liver by co-treatment of high fat diet (HFD) and sodium arsenite as compared to HFD alone, but no difference was observed between low fat diet groups [31]. Therefore, glycylglycine, glycine, hypotaurine and cholic acid may be promising candidate marker of arsenic toxicity. Furthermore, these four metabolites have been detected in urine and/or plasma of human and rat [32–34], making non-invasive assessment possible.

Ingenuity Pathway Analysis revealed liver damages at molecular level

To infer the possible biological impact associated with the metabolic changes, the KEGG IDs and log₂ FC of 57 identified metabolites (VIP>1) were submitted to IPA for Metabolomic analysis. IPA predicted effects on Disease and Bio Functions and Tox Functions (Fig 2A, S2 Table). In the aspect of Disease and Disorders, top categories were Cancer and diseases in gastrointestinal and hepatic systems, suggesting damages to the liver. Nervous System Development and Function was also significant ($p = 7.78E-08$), consistent with the neurotoxic effects reported in zebrafish embryo/larvae [17]. In Molecular and Cellular Functions, Amino Acid Metabolism was altered with the top significance, followed by molecular transport (of small carbohydrates and lipids). Interestingly, a few annotation terms of Lipid Metabolism were also affected, including concentration of fatty acid, sterol, and cholesterol; and conversion of lipids. Arsenic-induced changes in lipid metabolism genes in zebrafish have been reported before [23]. Taken

Table 1. List of 34 potential metabolic markers for arsenate toxicity.

Metabolite Name	KEGG	Kovats RI	Fiehn RI	VIP	Fold Change	p value	Status
Cholic acid	C00695	3418.5	1110668	1.79	1.51	0.0021	probable
Unknown (peak 311)		3436.6	1113712	1.69	1.41	0.0044	
Ursodeoxycholic acid	C07880	3301.8	1094022	1.64	1.31	0.0083	probable
Chenodeoxycholic acid	C02528	3344.6	1099922	1.64	1.33	0.0087	probable
Unknown (peak 152)		1710.5	583073	1.62	1.90	0.0037	
Unknown (peak 8)		1023.4	220331	1.61	1.66	0.0118	
Unknown (peak 314)		3523.3	1128266	1.59	1.32	0.0150	
Mannose	C00159	1953.8	686570	1.50	1.31	0.0113	probable
2-Ketovaline	C00141	1153.8	291985	1.47	1.75	0.0151	probable
Unknown (peak 189)		1943.8	682483	1.46	2.14	0.0252	
Unknown (peak 67)		1253.3	349182	1.39	1.86	0.0241	
Unknown (peak 59)		1219.7	329155	1.39	1.43	0.0266	
Gluconic acid	C00257	1946.4	683531	1.38	1.49	0.0246	probable
Unknown (peak 234)		2201.3	809327	1.36	1.45	0.0280	
Succinic acid	C00042	1305.7	380427	1.28	1.67	0.0429	confirmed
Unknown (peak 63)		1238.9	340611	1.28	2.08	0.0434	
Unknown (peak 140)		1619.3	541619	1.26	1.76	0.0482	
Glycylglycine	C02037	1814	629175	1.92	0.57	0.0002	probable
2-Oxovaleric acid	C06255	1111.3	268640	1.69	0.68	0.0029	probable
Myo-Inositol 1-phosphate	C01177	2487.3	885736	1.63	0.85	0.0218	probable
Unknown (peak 15)		1053.8	237000	1.62	0.60	0.0044	
Hypotaurine	C00519	1602.4	533953	1.60	0.63	0.0130	probable
3-hydroxybutanoic acid	C01089	1158.5	294592	1.60	0.59	0.0117	confirmed
Unknown (peak 4)		1002.7	208915	1.57	0.40	0.0084	
Palmitoleic acid	C08362	2016.7	711860	1.53	0.44	0.0193	confirmed
Glycine	C00037	1113.1	269628	1.52	0.69	0.0198	confirmed
Unknown (peak 101)		1431.3	447764	1.51	0.40	0.0213	
Ethanolamine	C00189	1243.3	343218	1.48	0.81	0.0447	confirmed
2-Aminobutanoate	C02356	1175.1	303717	1.47	0.56	0.0276	probable
Linoleic acid	C01595	2199.6	808238	1.46	0.62	0.0198	confirmed
Alpha-linolenic acid	C06427	2203.8	810927	1.46	0.44	0.0352	probable
Oleic acid	C00712	2208.5	813872	1.42	0.58	0.0280	probable
Unknown (peak 117)		1517.3	491580	1.37	0.72	0.0418	
Threonine	C00188	1294.5	373791	1.37	0.33	0.0447	confirmed

Potential markers were with VIP>1 in PLS-DA model and $p<0.05$ in Welch's t test.

doi:10.1371/journal.pone.0151225.t001

together, the output suggested that arsenic could damage the liver and affect the cellular transport and metabolism of amino acids and lipids. In terms of Hepatotoxicity predicted under Top Tox Functions, Liver Hyperplasia and Hepatocellular Carcinoma were the top predicted toxico-pathological outcomes, followed by Liver Steatosis and Liver Damage.

IPA also predicted 13 significantly altered canonical pathways ($p<0.005$, Fig 2B). The reduction of multiple amino acids led to significant predicted changes in pathways such as tRNA Charging and metabolism of specific amino acids (e.g. glycine biosynthesis/betaine degradation, alanine degradation/biosynthesis, and glutamate degradation via 4-aminobutyrate). Glutathione-mediated detoxification was also altered. An interesting pathway to note is FXR/

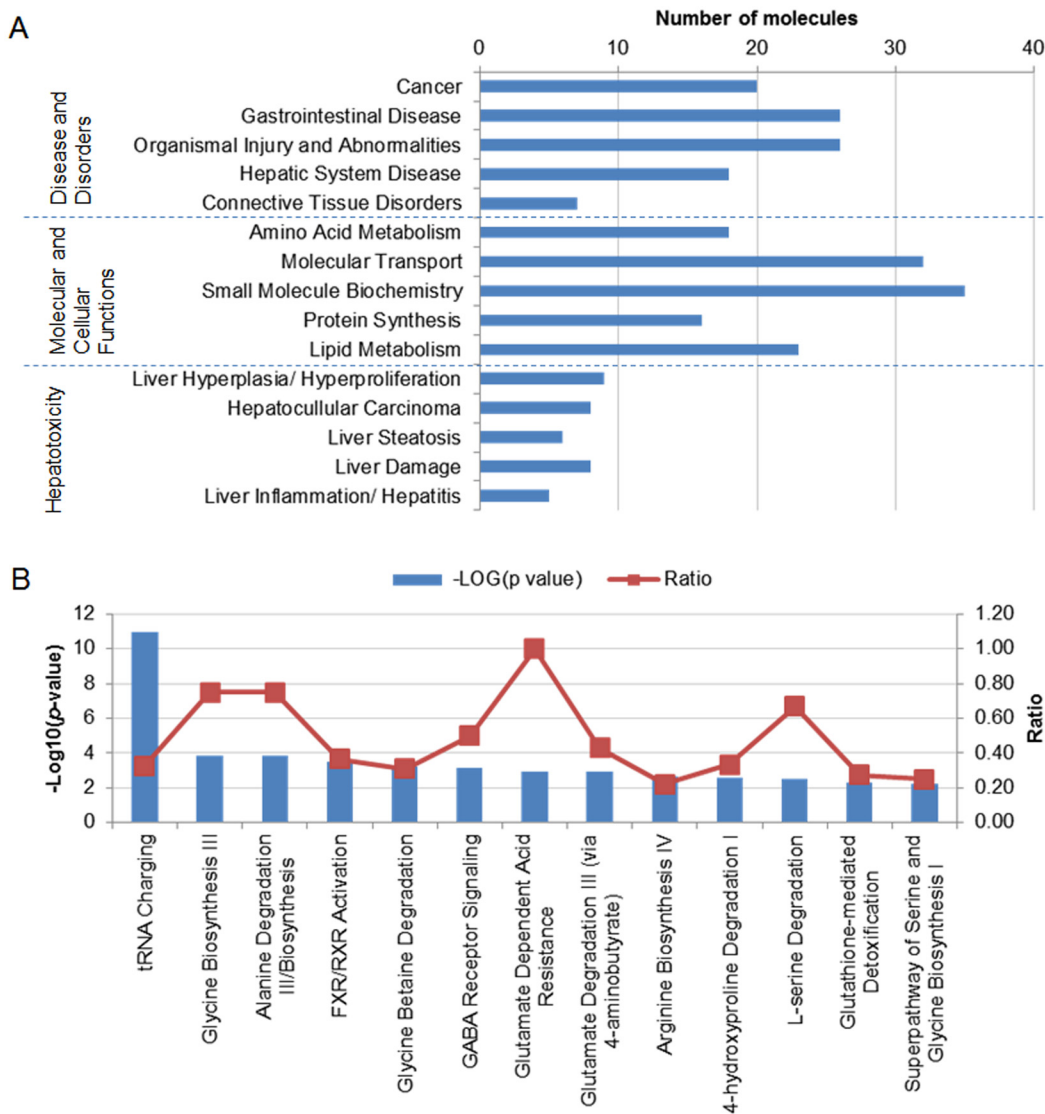


Fig 2. Effects of the metabolic alteration on Disease and Bio Functions and Tox Functions predicted by IPA ($p < 0.05$). (A) The top five entries in three aspects of biological impact: Disease and Disorders, Molecular and Cellular Functions, and Hepatotoxicity. (B) Top altered canonical pathways predicted by IPA ($p < 0.005$). The p values were calculated using Fischer's exact test determining the probability that the association between the genes in the data set and the canonical pathway was due to chance alone. The ratios were calculated based on the number of genes from the data set that mapped to the pathway and the total number of genes in the pathway.

doi:10.1371/journal.pone.0151225.g002

RXR activation, which plays a role in modulation of bile acid homeostasis, lipid metabolism and glucose [35].

Histological examination showed that As weakened cellular organization, changed content of glycogen and lipid, and induced apoptosis

Histological analyses were performed to validate liver damages predicted in IPA. In fact, at the end of arsenate exposure, livers of As-treated fish appeared to be softer and more watery than those of control fish, indicating compromised integrity of the tissue. In H&E stained sections, control hepatocytes were homogenous in size and highly organized into a two-cell

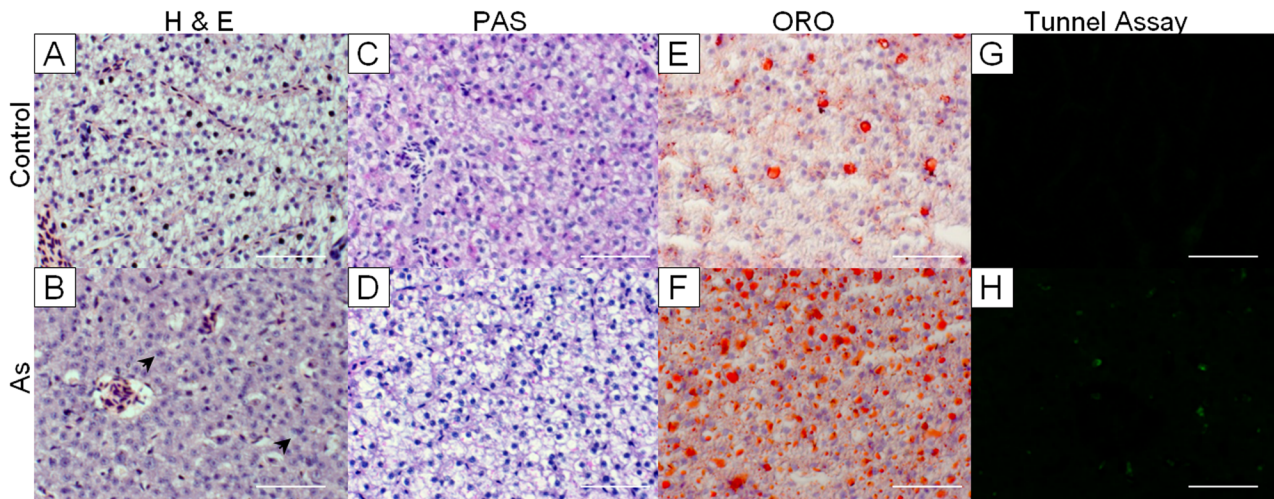


Fig 3. Histological examinations of liver sections. (A-B) H&E staining revealed changes in cellular organization, cytoplasmic volume, and nuclei morphology in treated group (lower panel) as compared to control (upper panel). (C-D) ORO staining showed marked accumulation of lipid droplets in As group. (E-F) Glycogen depletion in the As group was evident with PAS staining. (G-H) Increased apoptotic cells (stained with green fluorescence) were observed in the As group. Magnification: 400x. Arrow: binucleated cells. Scale bars: 50µm.

doi:10.1371/journal.pone.0151225.g003

plates (Fig 3A). In contrast, hepatocytes in treated group were less organized and more heterogeneous in size. Nuclei were generally larger and slightly more variable in size than those in controls and binucleated cells were occasionally observed. These changes were consistent with previous observations [24]. Empty spots of various sizes were observed in As-treated samples (Fig 3B), which might be a result of cell death and/or accumulation of fats as both of them showed significant increases (see Fig 3E–3H). Eosin stained area increased in the As group, suggesting reduction of glycogen contents. This was confirmed by PAS staining, where control livers were all stained reddish (Fig 3C) but at least 60% (6/9) of treated liver were less stained (Fig 3D). Depletion of liver glycogen after arsenate exposure has been described before and it was thought to be a result of glycogen mobilization induced by toxicant stress [24]. An additional cause may be the reduction of pentavalent arsenic to trivalent form in liver [36] by glycogen phosphorylase, a reaction that is coupled to glycogenolysis [37]. The product of glycogenolysis, Glucose-1-phosphate (G1P), can be converted into Glucose-6-phosphate (G6P) for glycolysis.

ORO staining was performed to visualize lipid content. Orange-red fat droplets were markedly increased in As group (Fig 3E and 3F). Interestingly, IPA predicted a negative z score on liver steatosis (S2 Table) based on the increase of fructose and reduction of oleic acid, glutamic acid, methionine, phenylalanine, and tryptophan. This seemed to be contradictory to the ORO staining results. While reduction of the amino acids and a fatty acid might be related to decreased lipogenesis, increase of fructose can increase glucose influx and contribute to *de novo* lipogenesis and insulin resistance [38], which could contribute to accumulation of hepatic fats. Liver stores excess lipids as neutral lipid esters in droplets to prevent lipotoxicity [39]. ORO stains cholesteryl esters and neutral lipids, including triglycerides (TGs) and diglycerides (DGs), on frozen tissue sections [40]. It is possible that upon arsenic treatment, fat accumulates in the liver as lipid esters in droplets while free fatty acids reduce or remain unchanged. In fact, two saturated fatty acids (octadecanoic acid and tetradecanoic acid) and one trans unsaturated fatty acid (elaidic acid) detected were not significantly altered (S3 Table). These differential effects of sodium arsenate on fatty acids are partially consistent with a recent study in male rats [41]. After 10 months of exposure to arsenic, cis unsaturated fatty acids significantly decreased,

while saturated fatty acids and trans unsaturated fatty acid increased in treated group. Differential effects of saturated and unsaturated fatty acids on fatty liver progression have been reported before but underlying mechanisms remain unclear [42]. As excretion of bile acids is the primary way of cholesterol elimination [43], the accumulation of bile acids observed indicated compromised removal of cholesterol, which could in turn contribute to lipid accumulation.

Tunnel assay revealed notable increase of apoptotic cells in the treated livers (Fig 3G and 3H), confirming the indication of tissue damages by IPA. Arsenic-induced apoptosis has long been described and considered to be a result of a sequential event: early decrease in cellular mitochondria potential, increase of reactive oxygen species (ROS), and finally activation of caspase-3 dependent apoptosis pathway resulting DNA fragmentation [44–47]. These histopathological alterations confirmed that the current exposure is sufficient to cause some cellular damages in liver and apoptosis of a small percentage of hepatocytes. However, the liver impairments were still mild, as there were no severe features observed, such as inflammation, massive cell death, marked ballooning, cirrhosis and polymorphism of cell size and nuclei size (tumour features) [48–50]. Beside, accumulation of lipid droplets is reversible before fibrosis and cirrhosis have developed [50]. In fact, fibrosis was not observed in picosirius red staining of the liver sections (data not shown).

Conventional liver function tests did not indicate liver damages

To further assess the liver damages, we performed two conventional liver function tests, plasma bilirubin assay and ALT activity assay. Plasma bilirubin level can be altered by conditions such as hepatitis, biliary obstruction and cirrhosis, while plasma ALT level elevates if integrity of hepatocytes is compromised [51]. Five biological replicates, each a pooled sample from 3–6 fish, were used in all assays (Fig 4).

Unconjugated bilirubin is a product of heme catabolism, which can be transported to the liver and conjugated to glucuronides by UDP-glucuronosyltransferases (UGTs) to form conjugated bilirubin. Conjugated bilirubin is secreted into bile and excreted or recycled to plasma, accounting for a minute percentage of total plasma bilirubin [52]. Results showed that total plasma protein was elevated by about 35% ($p < 0.01$) in the As group (Fig 4A). Total bilirubin in the As group was 6.42 ± 5.43 mg/dL, significantly higher ($p < 0.05$) than the value of 1.73

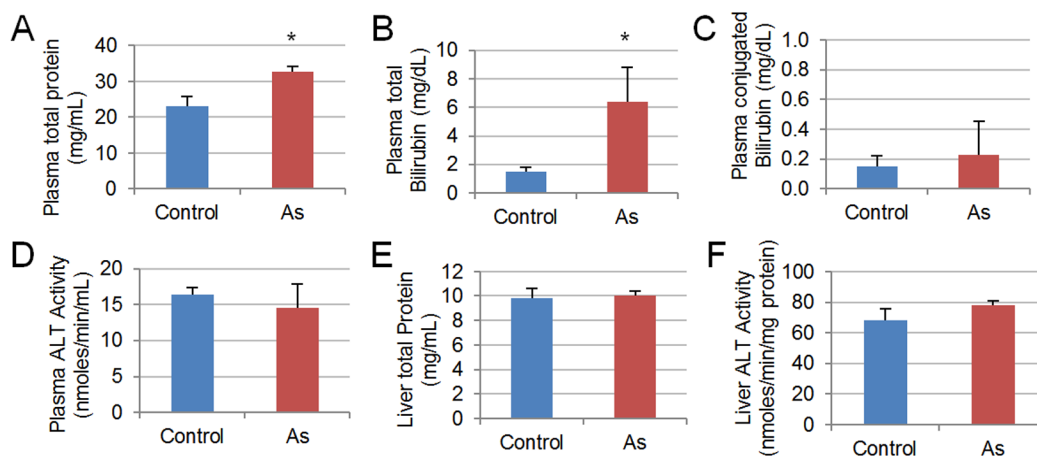


Fig 4. Liver function tests by Bilirubin assay (A-C) and ALT assay (D-F). Total protein content (A) and total bilirubin (B) were significantly higher in plasma of As-treated fish as compared to control, with $p = 0.008$ and $p = 0.037$ respectively. Direct bilirubin (C) and plasma ALT activity (D) remained normal ($p > 0.3$). No significant change was found in total protein concentration (E) or ALT activity (F) of liver ($p > 0.1$). Five biological replicates were used for each assay and statistical test used was one-tailed student t -test.

doi:10.1371/journal.pone.0151225.g004

± 0.94 mg/dL in controls (Fig 4B). Conjugated bilirubin was similarly low or absent in both As (0.23 ± 0.51 mg/dL) and control (0.13 ± 0.15 mg/dL) samples (Fig 4C), indicating absence of bile duct obstruction, hepatitis or cirrhosis [51]. An increase in unconjugated bilirubin is likely a result of hemolysis and/or ineffective bilirubin conjugation. Bilirubin conjugation in zebrafish has not been well studied. A recent *in vitro* study has shown that only *ugt1* family could conjugate bilirubin, among which *ugt1b7* has the highest catalytic activity and it is detected in the liver [53]. However, in a liver transcriptomic profile we obtained under the same As exposure conditions, none of the *ugt1* genes is deregulated [3]. Furthermore, there has been reports of hemolytic anaemia in individuals with acute [54] or chronic [55] exposure. Thus, it is more probable that the elevation of unconjugated bilirubin was due to increased hemolysis in blood.

ALT is highly enriched in the liver and liver injuries lead to increase in its serum concentration [51]. Unexpectedly, plasma ALT activity was not significantly altered ($p > 0.3$, Fig 4D). Total protein and ALT activity were also quantified in liver samples and no significant change was observed (Fig 4E and 4F). Taken together, the analysis suggested there was probably no severe damage of liver. It should be pointed out that, plasma used in these function assays were obtained from fish exposure to 15 ppm and greater changes might be observable at 20 ppm. However, exposure to arsenic does not necessarily led to significant changes in plasma live function assays. In a study on a population of west Bengal of India exposure to different levels of arsenic, serum bilirubin was elevated in total exposed individuals but no significance was detected in dose-response tests [56]. ALT activity in plasma were frequently elevated after arsenic exposure in human [56, 57] or animal models [58, 59]; however, such changes are usually significant only under very high concentrations [57, 60] or prolonged exposure of weeks to months [61–63]. Thus, the arsenate exposure in this study was probably not sufficient to induce severe liver damages. This is further supported by the absence of histopathological evidence for severe liver damages as described earlier. In addition, it has been recently recognized that, ALT level may remain normal in patients with non-alcoholic fatty liver disease, viral hepatitis and some metabolic disorders [64].

Arsenate altered metabolic networks of bile acid regulation, glycolysis, and fatty acid metabolism

The experimental evidence, knowledge-based data mining of biological pathways and associated biological interpretations together indicated that, the toxicity exerted by arsenate involved bile acid homeostasis, amino acid metabolism, glycogen metabolism and lipid metabolism. We further examined a network focusing glycogenolysis and glycolysis pathway, which is central to energy metabolism and also related to amino acid and lipid metabolism, with reference to relevant mRNA changes from a transcriptomic profile of arsenate exposure we previously obtained using the same exposure conditions [3]. The network structure was modified from IPA Target Explorer (<https://targetexplorer.ingenuity.com/index.htm>).

The observation of arsenic-induced glycogenolysis and glycolysis intermediates with concurrent increase in pyruvate has been reported before [65]. Besides, mechanism of arsenic toxicity has been postulated to include inhibition of energy-linked functions in mitochondria, direct inhibition of pyruvate dehydrogenase, and disruption of enzymatic reaction involving glyceraldehyde 3-phosphate dehydrogenase (GAPDH) [36]. As shown in Fig 5, the first and last few steps of glycolysis seemed to be promoted while intermediate steps were down-regulated. In addition to increased glucose, glycogenolysis (evident in the PAS staining) and increased conversion of G1P to G6P together provided more input to glycolysis, which was supported by the up-regulation of transcripts for key enzymes in the process (*pygb*, *pgm3* and *pybl*). However, G6P seemed to be channeled to pentose phosphate pathway (PPP) and

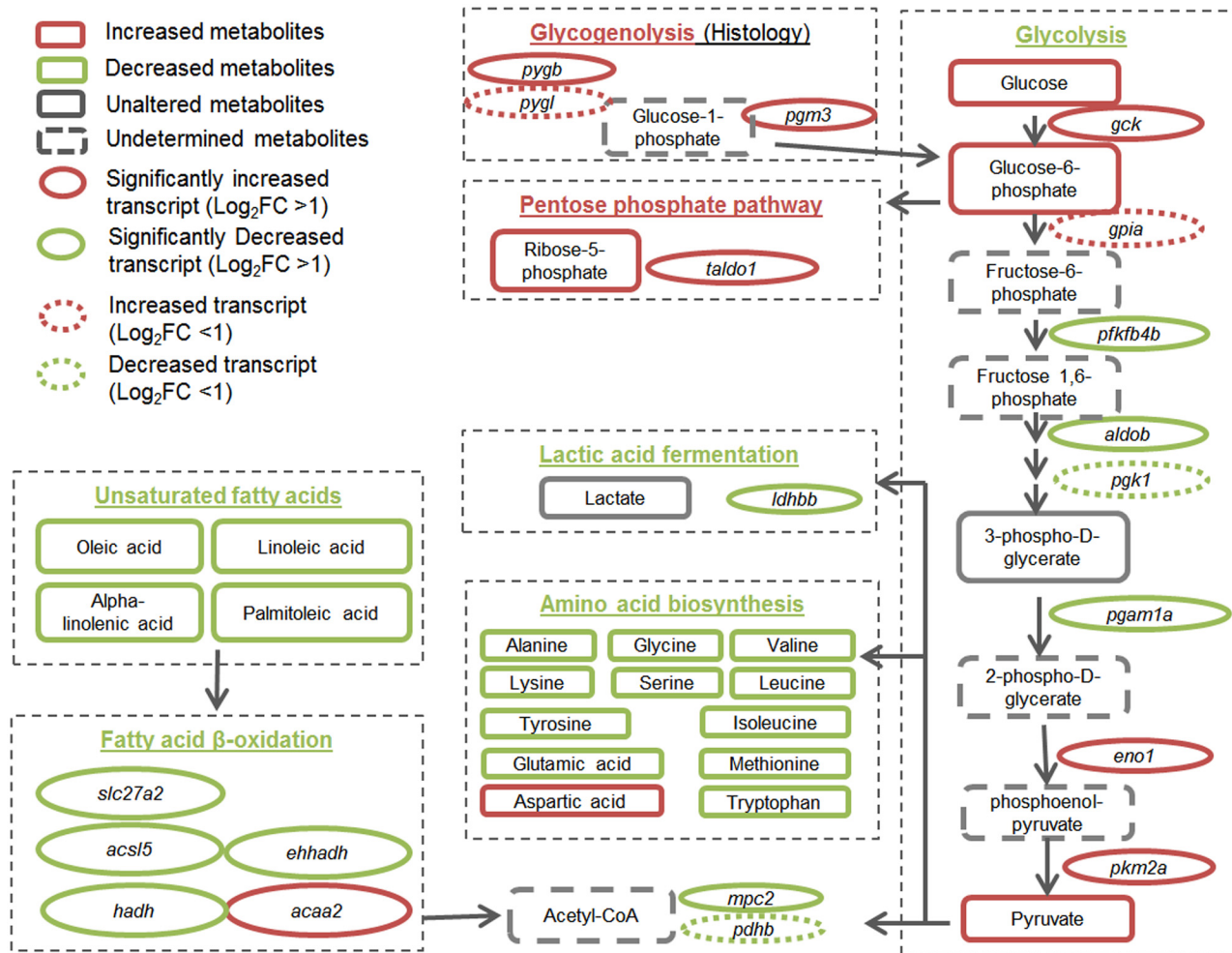


Fig 5. Network of glycolysis, glycogen metabolism and fatty acid metabolism constructed based on metabolic changes found in this study and mRNA changes reported in our previous transcriptomic study [3]. Gene names: *acaa2*, acetyl-CoA acyltransferase 2; *acsI5*, acyl-CoA synthetase long-chain family member 5; *aldob*, aldolase b, fructose-bisphosphate; *ehhadh*, enoyl-Coenzyme A, hydratase/3-hydroxyacyl Coenzyme A dehydrogenase; *eno1*, enolase 1, (alpha); *gck*, glucokinase (hexokinase 4); *gpiA*, glucose phosphate isomerase a; *hadh*, hydroxyacyl-Coenzyme A dehydrogenase; *ldhbb*, lactate dehydrogenase Bb; *mpc2*, mitochondrial pyruvate carrier 2; *pfkfb4b* (*pfkfb4l*), 6-phosphofructo-2-kinase/fructose-2,6-bisphosphatase 4b; *pgam1a*, phosphoglycerate mutase 1a; *pgm3*, phosphoglucomutase 3; *pgk1*, phosphoglycerate kinase 1; *pkm2a*, pyruvate kinase, muscle, a; *pygb*, phosphorylase, glycogen; brain; *pygl*, phosphorylase, glycogen, liver; *slc27a2*, solute carrier family 27 (fatty acid transporter), member 2; *taldo1*, transaldolase 1.

doi:10.1371/journal.pone.0151225.g005

resulted in increase in ribose-5-phosphate (R5P), a substrate for synthesis of ribonucleotides. The PPP is also a major source of NADPH, which is a scavenger of ROS and is required for fatty acid synthesis [66]. The transcriptomic profile showed no increase in fatty acid or ribonucleotide synthesis pathway, so this channeling to PPP may be favored to counter the oxidative stress induced by arsenic. Interestingly, pyruvate was built up and none of the downstream utilization seemed to be activated: transcript of the key enzyme *ldhbb* for lactic acid fermentation was down-regulated; amino acids biosynthesis seemed to be impaired; and transport of pyruvate to mitochondria and to acetyl-CoA were both inhibited (down-regulation of *mpc2* and *pdhb*). The insufficient utilization of pyruvate might be a protective response of the cell to avoid generation of more ROS in the catabolism of acetyl-CoA. Not only the conversion of pyruvate to acetyl-CoA was reduced, oxidation of fatty acid at mitochondria was also down-regulated at the transcript level, suggesting a reduction in another source of acetyl-CoA to fuel

the TCA cycle for energy production. It is also noted that genes coding for enzymes that hydrolyze TGs and cholesteryl esters (*cel.1* and *cel1*) were also down-regulated, which may partially account for the reduction in free unsaturated fatty acids and increased lipid droplets.

Interestingly, the changes in glycolysis pathway partially resembled Warburg effect, a metabolic feature commonly observed in many cancer cells, where there is enhanced glycolysis and lactate fermentation even in presence of sufficient oxygen [67]. It has been reported that Warburg effect provides cancer cells with growth advantages (increased building blocks for biosynthesis and reduced oxidative stress) [68]. Rate limiting enzymes in glycolysis and lactate fermentation pathway, including glucokinases, pyruvate kinase and lactate dehydrogenase, are up-regulated in Warburg effect; in addition, PPP and TCA cycle are also enhanced [69, 70]. In arsenate treated liver, we observed increased transcripts of glucokinase (*gck*) and pyruvate kinase (*pkm2a*), increased G6P and pyruvate, and increased activity of PPP. In particular, *pkm2a* is coding for the M2 isoform of pyruvate kinases, an isoform whose expression is not normally found in the liver but is elevated in cancer cells [71–73]. The main difference from Warburg effect was the lack of enhanced lactate fermentation, based on the decrease of lactate as well as down-regulation of *ldhbb*. Arsenic-induced Warburg effect has been reported in only one *in vitro* study [74], where sodium arsenite increased glycolysis and lactate fermentation in human bronchial epithelial cells. Interestingly, while transcripts for enzymes in all glycolytic steps increased at 2 weeks and 4 weeks of exposure, transcripts of some enzymes at the intermediate steps (eg. ENO3 and PGK2) decreased after 1 week of exposure while transcripts for GCK. This is consistent with our observations described. We postulate that, with prolonged exposure, arsenate might also induce Warburg effect as a secondary consequence of direct toxic effects, which could in turn contribute to carcinogenesis.

Taken together, we hypothesize that cellular perturbations in liver by acute exposure to sodium arsenate may involve the following aspects: (1) glycogen is rapidly depleted, with at least some of the end products entering glycolysis; (2) G6P is mainly channeled to PPP, presumably for production of NADPH to counter the oxidative stress induced by arsenate; (3) pyruvate transport to mitochondria and further utilization are impaired and energy production is compromised, which could be a result of enzyme inhibition or a protective response to reduce generation of ROS; (4) various free amino acids are decreased; (5) bile acids accumulate in liver (risk of cholestasis); (6) cellular fatty acid composition is affected and lipid droplets dramatically increased, which could be a result of TG built up and compromised lipoprotein metabolism. The alterations in glycolysis pathway partially resemble Warburg effect, which could be a contributing factor of arsenate-induced carcinogenesis. In addition, this study indicated that metabolic changes could be sensitive markers to reflect mild liver impairments (e.g. induced by arsenic exposure), which may not be detectable by conventional liver function tests such as Bilirubin assay and ALT assay.

Supporting Information

S1 Fig. Hierarchical clustering of samples using peak areas of subset of seven metabolites.

Peak areas were quantile-normalized and standardized to respective mean value of each metabolite among all samples. Hierarchical clustering was performed using Pearson correlation method without mean centering.

(TIF)

S2 Fig. Standard curve of calibrator for bilirubin assay in recommended assay setup and the scaled-down setup used in this study. Limited by the minute amount of plasma collectable from zebrafish, assay was scaled down (2 μ L plasma in 125 μ L assay mixture) from the manu-

facturer's protocol (50 μ L in 250 μ L assay mixture). The linearity was conserved across the two assay setups and thus the use of the modified assay setup was valid.

(TIF)

S1 Table. Complete list of 57 altered metabolites (contributing to group separation in PLS-DA model) identified by GC/MS.

(DOCX)

S2 Table. IPA predicted effects of the metabolic alteration on Disease and Biofunctions and Tox Functions. ($p < 0.01$ and #molecular ≥ 3)

(XLSX)

S3 Table. List of unaltered metabolites (not contributing to group separation in PLS-DA modeling) identified by GC/MS.

(DOCX)

Author Contributions

Conceived and designed the experiments: CL PL SHL ECYC ZG. Performed the experiments: CL PL. Analyzed the data: CL YMT ECYC ZG. Contributed reagents/materials/analysis tools: CL YMT SHL ECYC. Wrote the paper: CL SHL ECYC ZG.

References

1. Chakraborti D. Arsenic: Occurrence in Groundwater. In: Nriagu JO, editor. Encyclopedia of Environmental Health. Burlington: Elsevier; 2011. p. 165–80.
2. Marchiset-Ferlay N, Savanovitch C, Sauvant-Rochat MP. What is the best biomarker to assess arsenic exposure via drinking water? Environ Int. 2012; 39(1):150–71. doi: [10.1016/j.envint.2011.07.015](https://doi.org/10.1016/j.envint.2011.07.015) PMID: [22208756](https://pubmed.ncbi.nlm.nih.gov/22208756/).
3. Xu H, Lam SH, Shen Y, Gong Z. Genome-wide identification of molecular pathways and biomarkers in response to arsenic exposure in zebrafish liver. PLoS one. 2013; 8(7):e68737. doi: [10.1371/journal.pone.0068737](https://doi.org/10.1371/journal.pone.0068737) PMID: [23922661](https://pubmed.ncbi.nlm.nih.gov/23922661/); PubMed Central PMCID: PMC3726666.
4. Bolt H. Arsenic: an ancient toxicant of continuous public health impact, from Iceman Ötzi until now. Arch Toxicol. 2012; 86(6):825–30. doi: [10.1007/s00204-012-0866-7](https://doi.org/10.1007/s00204-012-0866-7) PMID: [22638732](https://pubmed.ncbi.nlm.nih.gov/22638732/)
5. Lage CR, Nayak A, Kim CH. Arsenic ecotoxicology and innate immunity. Integr Comp Biol. 2006; 46(6):1040–54. doi: [10.1093/icb/icl048](https://doi.org/10.1093/icb/icl048) PMID: [21672806](https://pubmed.ncbi.nlm.nih.gov/21672806/).
6. Hughes MF, Beck BD, Chen Y, Lewis AS, Thomas DJ. Arsenic exposure and toxicology: a historical perspective. Toxicol Sci. 2011; 123(2):305–32. doi: [10.1093/toxsci/kfr184](https://doi.org/10.1093/toxsci/kfr184) PMID: [21750349](https://pubmed.ncbi.nlm.nih.gov/21750349/); PubMed Central PMCID: PMC3179678.
7. Moore LE, Karami S, Steinmaus C, Cantor KP. Use of OMIC technologies to study arsenic exposure in human populations. Environ Mol Mutagen. 2013; 54(7):589–95. doi: [10.1002/em.21792](https://doi.org/10.1002/em.21792) PMID: [23893652](https://pubmed.ncbi.nlm.nih.gov/23893652/).
8. Dudka I, Kossowska B, Senhadri H, Latajka R, Hajek J, Andrzejak R, et al. Metabonomic analysis of serum of workers occupationally exposed to arsenic, cadmium and lead for biomarker research: a preliminary study. Environ Int. 2014; 68:71–81. doi: [10.1016/j.envint.2014.03.015](https://doi.org/10.1016/j.envint.2014.03.015) PMID: [24713610](https://pubmed.ncbi.nlm.nih.gov/24713610/).
9. Garcia-Sevillano MA, Garcia-Barrera T, Navarro-Roldan F, Montero-Lobato Z, Gomez-Ariza JL. A combination of metallomics and metabolomics studies to evaluate the effects of metal interactions in mammals. Application to Mus musculus mice under arsenic/cadmium exposure. J Proteomics. 2014; 104:66–79. doi: [10.1016/j.jprot.2014.02.011](https://doi.org/10.1016/j.jprot.2014.02.011) PMID: [24549004](https://pubmed.ncbi.nlm.nih.gov/24549004/).
10. Lu K, Abo RP, Schlieper KA, Graffam ME, Levine S, Wishnok JS, et al. Arsenic exposure perturbs the gut microbiome and its metabolic profile in mice: an integrated metagenomics and metabolomics analysis. Environmental health perspectives. 2014; 122(3):284–91. doi: [10.1289/ehp.1307429](https://doi.org/10.1289/ehp.1307429) PMID: [24413286](https://pubmed.ncbi.nlm.nih.gov/24413286/); PubMed Central PMCID: PMC3948040.
11. Garcia-Sevillano MA, Garcia-Barrera T, Navarro F, Gomez-Ariza JL. Analysis of the biological response of mouse liver (Mus musculus) exposed to As₂O₃ based on integrated -omics approaches. Metallomics. 2013; 5(12):1644–55. doi: [10.1039/c3mt00186e](https://doi.org/10.1039/c3mt00186e) PMID: [24091382](https://pubmed.ncbi.nlm.nih.gov/24091382/).

12. Garcia-Sevillano MA, Jara-Biedma R, Gonzalez-Fernandez M, Garcia-Barrera T, Gomez-Ariza JL. Metal interactions in mice under environmental stress. *Biomaterials*. 2013; 26(4):651–66. doi: [10.1007/s10534-013-9642-2](https://doi.org/10.1007/s10534-013-9642-2) PMID: [23780566](https://pubmed.ncbi.nlm.nih.gov/23780566/).
13. Wu H, Liu X, Zhang X, Ji C, Zhao J, Yu J. Proteomic and metabolomic responses of clam *Ruditapes philippinarum* to arsenic exposure under different salinities. *Aquat Toxicol*. 2013; 136–137:91–100. doi: [10.1016/j.aquatox.2013.03.020](https://doi.org/10.1016/j.aquatox.2013.03.020) PMID: [23660018](https://pubmed.ncbi.nlm.nih.gov/23660018/).
14. Nagato EG, D'Eon J C, Lankadurai BP, Poirier DG, Reiner EJ, Simpson AJ, et al. (1)H NMR-based metabolomics investigation of *Daphnia magna* responses to sub-lethal exposure to arsenic, copper and lithium. *Chemosphere*. 2013; 93(2):331–7. doi: [10.1016/j.chemosphere.2013.04.085](https://doi.org/10.1016/j.chemosphere.2013.04.085) PMID: [23732010](https://pubmed.ncbi.nlm.nih.gov/23732010/).
15. Stegeman JJ, Goldstone JV, Hahn ME. Perspectives on zebrafish as a model in environmental toxicology. *Fish Physiology*. 2010; 29:367–439. doi: [10.1016/s1546-5098\(10\)02910-9](https://doi.org/10.1016/s1546-5098(10)02910-9)
16. Li D, Lu C, Wang J, Hu W, Cao Z, Sun D, et al. Developmental mechanisms of arsenite toxicity in zebrafish (*Danio rerio*) embryos. *Aquat Toxicol*. 2009; 91(3):229–37. doi: [10.1016/j.aquatox.2008.11.007](https://doi.org/10.1016/j.aquatox.2008.11.007) PMID: [19110324](https://pubmed.ncbi.nlm.nih.gov/19110324/).
17. Ma Y, Zhang C, Gao XB, Luo HY, Chen Y, Li HH, et al. Folic acid protects against arsenic-mediated embryo toxicity by up-regulating the expression of Dvr1. *Sci Rep*. 2015; 5:16093. doi: [10.1038/srep16093](https://doi.org/10.1038/srep16093) PMID: [26537450](https://pubmed.ncbi.nlm.nih.gov/26537450/); PubMed Central PMCID: [PMC4633590](https://pubmed.ncbi.nlm.nih.gov/pmc/PMC4633590/).
18. McCollum CW, Hans C, Shah S, Merchant FA, Gustafsson JA, Bondesson M. Embryonic exposure to sodium arsenite perturbs vascular development in zebrafish. *Aquat Toxicol*. 2014; 152:152–63. doi: [10.1016/j.aquatox.2014.04.006](https://doi.org/10.1016/j.aquatox.2014.04.006) PMID: [24768856](https://pubmed.ncbi.nlm.nih.gov/24768856/).
19. Mattingly CJ, Hampton TH, Brothers KM, Griffin NE, Planchart A. Perturbation of defense pathways by low-dose arsenic exposure in zebrafish embryos. *Environ Health Perspect*. 2009; 117(6):981–7. doi: [10.1289/ehp.0900555](https://doi.org/10.1289/ehp.0900555) PMID: [19590694](https://pubmed.ncbi.nlm.nih.gov/19590694/); PubMed Central PMCID: [PMC2702417](https://pubmed.ncbi.nlm.nih.gov/pmc/PMC2702417/).
20. Nayak AS, Lage CR, Kim CH. Effects of low concentrations of arsenic on the innate immune system of the zebrafish (*Danio rerio*). *Toxicol Sci*. 2007; 98(1):118–24. doi: [10.1093/toxsci/kfm072](https://doi.org/10.1093/toxsci/kfm072) PMID: [17400579](https://pubmed.ncbi.nlm.nih.gov/17400579/).
21. Hamdi M, Sanchez MA, Beene LC, Liu Q, Landfear SM, Rosen BP, et al. Arsenic transport by zebrafish aquaglyceroporins. *BMC Mol Biol*. 2009; 10:104. doi: [10.1186/1471-2199-10-104](https://doi.org/10.1186/1471-2199-10-104) PMID: [19939263](https://pubmed.ncbi.nlm.nih.gov/19939263/); PubMed Central PMCID: [PMC2788550](https://pubmed.ncbi.nlm.nih.gov/pmc/PMC2788550/).
22. Liu C, Xu H, Lam SH, Gong Z. Selection of Reliable Biomarkers from PCR Array Analyses Using Relative Distance Computational Model: Methodology and Proof-of-Concept Study. *PLoS One*. 2013; 8(12): e83954. doi: [10.1371/journal.pone.0083954](https://doi.org/10.1371/journal.pone.0083954)
23. Carlson P, Van Beneden RJ. Arsenic exposure alters expression of cell cycle and lipid metabolism genes in the liver of adult zebrafish (*Danio rerio*). *Aquat Toxicol*. 2013. doi: [10.1016/j.aquatox.2013.10.006](https://doi.org/10.1016/j.aquatox.2013.10.006) PMID: [24176670](https://pubmed.ncbi.nlm.nih.gov/24176670/).
24. Lam SH, Winata CL, Tong Y, Korzh S, Lim WS, Korzh V, et al. Transcriptome kinetics of arsenic-induced adaptive response in zebrafish liver. *Physiological Genomics*. 2006; 27(3):351–61. doi: [10.1152/physiolgenomics.00201.2005](https://doi.org/10.1152/physiolgenomics.00201.2005) WOS:000242340100015. PMID: [16882884](https://pubmed.ncbi.nlm.nih.gov/16882884/)
25. Chan EC, Pasikanti KK, Nicholson JK. Global urinary metabolic profiling procedures using gas chromatography-mass spectrometry. *Nat Protoc*. 2011; 6(10):1483–99. doi: [10.1038/nprot.2011.375](https://doi.org/10.1038/nprot.2011.375) PMID: [21959233](https://pubmed.ncbi.nlm.nih.gov/21959233/).
26. Lee J, Park J, Lim MS, Seong SJ, Seo JJ, Park SM, et al. Quantile normalization approach for liquid chromatography-mass spectrometry-based metabolomic data from healthy human volunteers. *Anal Sci*. 2012; 28(8):801–5. PMID: [22878636](https://pubmed.ncbi.nlm.nih.gov/22878636/).
27. Watanabe T, Hirano S. Metabolism of arsenic and its toxicological relevance. *Arch Toxicol*. 2013; 87(6):969–79. doi: [10.1007/s00204-012-0904-5](https://doi.org/10.1007/s00204-012-0904-5) PMID: [22811022](https://pubmed.ncbi.nlm.nih.gov/22811022/).
28. Kim JH, Kang JC. The arsenic accumulation and its effect on oxidative stress responses in juvenile rockfish, *Sebastes schlegelii*, exposed to waterborne arsenic (As³⁺). *Environ Toxicol Pharmacol*. 2015; 39(2):668–76. doi: [10.1016/j.etap.2015.01.012](https://doi.org/10.1016/j.etap.2015.01.012) PMID: [25818984](https://pubmed.ncbi.nlm.nih.gov/25818984/).
29. Bears H, Richards JG, Schulte PM. Arsenic exposure alters hepatic arsenic species composition and stress-mediated gene expression in the common killifish (*Fundulus heteroclitus*). *Aquat Toxicol*. 2006; 77(3):257–66. doi: [10.1016/j.aquatox.2005.12.008](https://doi.org/10.1016/j.aquatox.2005.12.008) PMID: [16445994](https://pubmed.ncbi.nlm.nih.gov/16445994/).
30. Allen T, Singhal R, Rana SVS. Resistance to oxidative stress in a freshwater fish *Channa punctatus* after exposure to inorganic arsenic. *Biol Trace Elem Res*. 98(1):63–72. doi: [10.1385/bter:98:1:63](https://doi.org/10.1385/bter:98:1:63) PMID: [15051901](https://pubmed.ncbi.nlm.nih.gov/15051901/)
31. Shi X, Wei X, Koo I, Schmidt RH, Yin X, Kim SH, et al. Metabolomic analysis of the effects of chronic arsenic exposure in a mouse model of diet-induced fatty liver disease. *J Proteome Res*. 2013. doi: [10.1021/pr400719u](https://doi.org/10.1021/pr400719u) PMID: [24328084](https://pubmed.ncbi.nlm.nih.gov/24328084/).

32. Aoki M, Konya Y, Takagaki T, Umemura K, Sogame Y, Katsumata T, et al. Metabolomic investigation of cholestasis in a rat model using ultra-performance liquid chromatography/tandem mass spectrometry. *Rapid Commun Mass Spectrom*. 2011; 25(13):1847–52. doi: [10.1002/rcm.5072](https://doi.org/10.1002/rcm.5072) WOS:000291593900008. PMID: [21638360](https://pubmed.ncbi.nlm.nih.gov/21638360/)
33. Patel DK, Ogunbona A, Notarianni LJ, Bennett PN. Depletion of Plasma Glycine and Effect of Glycine by Mouth on Salicylate Metabolism during Aspirin Overdose. *Hum Exp Toxicol*. 1990; 9(6):389–95. WOS:A1990EH28100006. PMID: [2271231](https://pubmed.ncbi.nlm.nih.gov/2271231/)
34. Sjövall J, Griffiths W, Setchell KR, Mano N, Goto J. Analysis of Bile Acids. In: Makin HLJ, Gower DB, editors. *Steroid Analysis*: Springer Netherlands; 2010. p. 837–966.
35. Wang YD, Chen WD, Moore DD, Huang W. FXR: a metabolic regulator and cell protector. *Cell research*. 2008; 18(11):1087–95. doi: [10.1038/cr.2008.289](https://doi.org/10.1038/cr.2008.289) PMID: [18825165](https://pubmed.ncbi.nlm.nih.gov/18825165/).
36. McIntyre DO, Linton TK. 6—Arsenic. In: Chris M. Wood APF, Colin JB, editors. *Fish Physiology*. Volume 31, Part B: Academic Press; 2011. p. 297–349.
37. Nemeti B, Gregus Z. Glutathione-dependent reduction of arsenate by glycogen phosphorylase a reaction coupled to glycogenolysis. *Toxicological sciences: an official journal of the Society of Toxicology*. 2007; 100(1):36–43. doi: [10.1093/toxsci/kfm211](https://doi.org/10.1093/toxsci/kfm211) PMID: [17693425](https://pubmed.ncbi.nlm.nih.gov/17693425/).
38. Basaranoglu M, Basaranoglu G, Sabuncu T, Senturk H. Fructose as a key player in the development of fatty liver disease. *World J Gastroenterol*. 2013; 19(8):1166–72. doi: [10.3748/wjg.v19.i8.1166](https://doi.org/10.3748/wjg.v19.i8.1166) WOS:000315521700003. PMID: [23482247](https://pubmed.ncbi.nlm.nih.gov/23482247/)
39. Krahmer N, Farese RV Jr., Walther TC. Balancing the fat: lipid droplets and human disease. *EMBO molecular medicine*. 2013; 5(7):905–15. doi: [10.1002/emmm.201100671](https://doi.org/10.1002/emmm.201100671) PMID: [23740690](https://pubmed.ncbi.nlm.nih.gov/23740690/); PubMed Central PMCID: PMC3721468.
40. Mehlem A, Hagberg CE, Muhl L, Eriksson U, Falkevall A. Imaging of neutral lipids by oil red O for analyzing the metabolic status in health and disease. *Nat Protoc*. 2013; 8(6):1149–54. doi: [10.1038/nprot.2013.055](https://doi.org/10.1038/nprot.2013.055) PMID: [23702831](https://pubmed.ncbi.nlm.nih.gov/23702831/).
41. Kharroubi W, Dhibi M, Haouas Z, Chreif I, Neffati F, Hammami M, et al. Effects of sodium arsenate exposure on liver fatty acid profiles and oxidative stress in rats. *Environ Sci Pollut Res Int*. 2014; 21(3):1648–57. doi: [10.1007/s11356-013-2057-3](https://doi.org/10.1007/s11356-013-2057-3) PMID: [23949113](https://pubmed.ncbi.nlm.nih.gov/23949113/).
42. de Wit NJW, Afman LA, Mensink M, Muller M. Phenotyping the effect of diet on non-alcoholic fatty liver disease. *J Hepatol*. 2012; 57(6):1370–3. WOS:000311771300030. doi: [10.1016/j.jhep.2012.07.003](https://doi.org/10.1016/j.jhep.2012.07.003) PMID: [22796155](https://pubmed.ncbi.nlm.nih.gov/22796155/)
43. Li Y, Jadhav K, Zhang Y. Bile acid receptors in non-alcoholic fatty liver disease. *Biochem Pharmacol*. 2013; 86(11):1517–24. doi: [10.1016/j.bcp.2013.08.015](https://doi.org/10.1016/j.bcp.2013.08.015) PMID: [23988487](https://pubmed.ncbi.nlm.nih.gov/23988487/); PubMed Central PMCID: PMC3925679.
44. Akao Y, Yamada H, Nakagawa Y. Arsenic-induced apoptosis in malignant cells in vitro. *Leuk Lymphoma*. 2000; 37(1–2):53–63. doi: [10.3109/10428190009057628](https://doi.org/10.3109/10428190009057628) WOS:000085706200004. PMID: [10721769](https://pubmed.ncbi.nlm.nih.gov/10721769/)
45. Woo SH, Park IC, Park MJ, Lee HC, Lee SWJ, Chun YJ, et al. Arsenic trioxide induces apoptosis through a reactive oxygen species-dependent pathway and loss of mitochondrial membrane potential in HeLa cells. *Int J Oncol*. 2002; 21(1):57–63. WOS:000176270500009. PMID: [12063550](https://pubmed.ncbi.nlm.nih.gov/12063550/)
46. Wang Y, Zhang Y, Yang L, Cai BZ, Li JP, Zhou Y, et al. Arsenic trioxide induces the apoptosis of human breast cancer MCF-7 cells through activation of caspase-3 and inhibition of HERG channels. *Exp Ther Med*. 2011; 2(3):481–6. doi: [10.3892/Etm.2011.224](https://doi.org/10.3892/Etm.2011.224) WOS:000289818200016. PMID: [22977528](https://pubmed.ncbi.nlm.nih.gov/22977528/)
47. Banerjee N, Banerjee M, Ganguly S, Bandyopadhyay S, Das JK, Bandyopadhyay A, et al. Arsenic-induced mitochondrial instability leading to programmed cell death in the exposed individuals. *Toxicology*. 2008; 246(2–3):101–11. doi: [10.1016/j.tox.2007.12.029](https://doi.org/10.1016/j.tox.2007.12.029) PMID: [18304716](https://pubmed.ncbi.nlm.nih.gov/18304716/).
48. Lefkowitz JH. Chapter 13—Liver Biopsy Histopathology. In: by E, Editor TDBLWPM, Zakim D, editors. *Zakim and Boyer's Hepatology (Fifth Edition)*. Edinburgh: W.B. Saunders; 2006. p. 205–34.
49. Torres DM, Harrison SA. Chapter 28—Nonalcoholic Fatty Liver Disease and Nonalcoholic Steatohepatitis. In: McNally PR, editor. *GI/Liver Secrets (Fourth Edition)*. Philadelphia: Mosby; 2010. p. 201–6.
50. Hubscher SG. Histological assessment of non-alcoholic fatty liver disease. *Histopathology*. 2006; 49(5):450–65. doi: [10.1111/j.1365-2559.2006.02416.x](https://doi.org/10.1111/j.1365-2559.2006.02416.x) WOS:000241524800001. PMID: [17064291](https://pubmed.ncbi.nlm.nih.gov/17064291/)
51. Giannini EG, Testa R, Savarino V. Liver enzyme alteration: a guide for clinicians. *CMAJ*. 2005; 172(3):367–79. doi: [10.1503/cmaj.1040752](https://doi.org/10.1503/cmaj.1040752) PMID: [15684121](https://pubmed.ncbi.nlm.nih.gov/15684121/); PubMed Central PMCID: PMC545762.
52. Levitt DG, Levitt MD. Quantitative assessment of the multiple processes responsible for bilirubin homeostasis in health and disease. *Clin Exp Gastroenterol*. 2014; 7:307–28. doi: [10.2147/CEG.S64283](https://doi.org/10.2147/CEG.S64283) PMID: [25214800](https://pubmed.ncbi.nlm.nih.gov/25214800/); PubMed Central PMCID: PMC4159128.

53. Wang Y, Huang H, Wu Q. Characterization of the zebrafish Ugt repertoire reveals a new class of drug-metabolizing UDP glucuronosyltransferases. *Mol Pharmacol*. 2014; 86(1):62–75. doi: [10.1124/mol.113.091462](https://doi.org/10.1124/mol.113.091462) PMID: [24728488](https://pubmed.ncbi.nlm.nih.gov/24728488/).
54. Correia N, Carvalho C, Frieos F, Araujo JP, Almeida J, Azevedo A. Haemolytic anaemia secondary to arsenic poisoning: a case report. *Cases journal*. 2009; 2:7768. doi: [10.4076/1757-1626-2-7768](https://doi.org/10.4076/1757-1626-2-7768) PMID: [19918480](https://pubmed.ncbi.nlm.nih.gov/19918480/); PubMed Central PMCID: PMC2769370.
55. Lee J-J, Kim Y-K, Cho S-H, Park K-S, Chung I-J, Cho D, et al. Hemolytic Anemia as a Sequela of Arsenic Intoxication Following Long-Term Ingestion of Traditional Chinese Medicine. *J Korean Med Sci*. 2004; 19(1):127–9. doi: [10.3346/jkms.2004.19.1.127](https://doi.org/10.3346/jkms.2004.19.1.127) PMC2822248. PMID: [14966354](https://pubmed.ncbi.nlm.nih.gov/14966354/)
56. Das N, Paul S, Chatterjee D, Banerjee N, Majumder NS, Sarma N, et al. Arsenic exposure through drinking water increases the risk of liver and cardiovascular diseases in the population of West Bengal, India. *BMC Public Health*. 2012; 12. Artn 639 doi: [10.1186/1471-2458-12-639](https://doi.org/10.1186/1471-2458-12-639) WOS:000308705100002.
57. Yoshimura Y, Endo Y, Shimoda Y, Yamanaka K, Endo G. Acute Arsenic Poisoning Confirmed by Speciation Analysis of Arsenic Compounds in the Plasma and Urine by HPLC-ICP-MS. *Journal Of Occupational Health*. 2011; 53(1):45–9. doi: [10.1539/Joh.L10108](https://doi.org/10.1539/Joh.L10108) WOS:000286912200006. PMID: [21123960](https://pubmed.ncbi.nlm.nih.gov/21123960/)
58. Patel HV, Kalia K. Role of hepatic and pancreatic oxidative stress in arsenic induced diabetic condition in Wistar rats. *J Environ Biol*. 2013; 34(2):231–6. PMID: [24620584](https://pubmed.ncbi.nlm.nih.gov/24620584/).
59. Vutukuru SS, Prabhath NA, Raghavender M, Yerramilli A. Effect of arsenic and chromium on the serum amino-transferases activity in Indian major carp, *Labeo rohita*. *Int J Environ Res Public Health*. 2007; 4(3):224–7. PMID: [17911661](https://pubmed.ncbi.nlm.nih.gov/17911661/); PubMed Central PMCID: PMC3731638.
60. Islam K, Haque A, Karim R, Fajol A, Hossain E, Salam KA, et al. Dose-response relationship between arsenic exposure and the serum enzymes for liver function tests in the individuals exposed to arsenic: a cross sectional study in Bangladesh. *Environmental Health*. 2011; 10. Artn 64 doi: [10.1186/1476-069x-10-64](https://doi.org/10.1186/1476-069x-10-64) WOS:000293342700001.
61. Wei L, Liao PQ, Wu HF, Li XJ, Pei FK, Li WS, et al. Metabolic profiling studies on the toxicological effects of realgar in rats by H-1 NMR spectroscopy. *Toxicol Appl Pharmacol*. 2009; 234(3):314–25. doi: [10.1016/j.taap.2008.11.010](https://doi.org/10.1016/j.taap.2008.11.010) WOS:000263253700006. PMID: [19073202](https://pubmed.ncbi.nlm.nih.gov/19073202/)
62. Nain S, Smits JEG. Pathological, immunological and biochemical markers of subchronic arsenic toxicity in rats. *Environ Toxicol*. 2012; 27(4):244–54. doi: [10.1002/Tox.20635](https://doi.org/10.1002/Tox.20635) WOS:000301346800007. PMID: [20725942](https://pubmed.ncbi.nlm.nih.gov/20725942/)
63. Guha Mazumder DN. Arsenic and liver disease. *J Indian Med Assoc*. 2001; 99(6):311, 4–5, 8–20. PMID: [11678619](https://pubmed.ncbi.nlm.nih.gov/11678619/).
64. Liu Z, Que S, Xu J, Peng T. Alanine aminotransferase-old biomarker and new concept: a review. *Int J Med Sci*. 2014; 11(9):925–35. doi: [10.7150/ijms.8951](https://doi.org/10.7150/ijms.8951) PMID: [25013373](https://pubmed.ncbi.nlm.nih.gov/25013373/); PubMed Central PMCID: PMC4081315.
65. Reichl FX, Szinicz L, Kreppel H, Forth W. Effect Of Arsenic on Carbohydrate-Metabolism after Single Or Repeated Injection In Guinea-Pigs. *Arch Toxicol*. 1988; 62(6):473–5. doi: [10.1007/Bf00288353](https://doi.org/10.1007/Bf00288353) WOS:A1988T561400013. PMID: [3250379](https://pubmed.ncbi.nlm.nih.gov/3250379/)
66. Patra KC, Hay N. The pentose phosphate pathway and cancer. *Trends Biochem Sci*. 2014; 39(8):347–54. doi: [10.1016/j.tibs.2014.06.005](https://doi.org/10.1016/j.tibs.2014.06.005) PMID: [25037503](https://pubmed.ncbi.nlm.nih.gov/25037503/); PubMed Central PMCID: PMC4329227.
67. Koppenol WH, Bounds PL, Dang CV. Otto Warburg's contributions to current concepts of cancer metabolism (vol 11, pg 325, 2011). *Nature Reviews Cancer*. 2011; 11(8):618-. doi: [10.1038/nrc3108](https://doi.org/10.1038/nrc3108) WOS:000292998200017.
68. Mikawa T, LLeonart ME, Takaori-Kondo A, Inagaki N, Yokode M, Kondoh H. Dysregulated glycolysis as an oncogenic event. *Cell Mol Life Sci*. 2015; 72(10):1881–92. doi: [10.1007/s00018-015-1840-3](https://doi.org/10.1007/s00018-015-1840-3) WOS:000353231300004. PMID: [25609364](https://pubmed.ncbi.nlm.nih.gov/25609364/)
69. Heiden MG, Cantley LC, Thompson CB. Understanding the Warburg Effect: The Metabolic Requirements of Cell Proliferation. *Science*. 2009; 324(5930):1029–33. doi: [10.1126/science.1160809](https://doi.org/10.1126/science.1160809) WOS:000266246700031. PMID: [19460998](https://pubmed.ncbi.nlm.nih.gov/19460998/)
70. Vaitheesvaran B, Xu J, Yee J, Lu QY, Go VL, Xiao GG, et al. The Warburg effect: a balance of flux analysis. *Metabolomics*. 2015; 11(4):787–96. doi: [10.1007/s11306-014-0760-9](https://doi.org/10.1007/s11306-014-0760-9) WOS:000356538000004. PMID: [26207106](https://pubmed.ncbi.nlm.nih.gov/26207106/)
71. Yang WW, Lu ZM. Regulation and function of pyruvate kinase M2 in cancer. *Cancer Lett*. 2013; 339(2):153–8. doi: [10.1016/j.canlet.2013.06.008](https://doi.org/10.1016/j.canlet.2013.06.008) WOS:000325304000001. PMID: [23791887](https://pubmed.ncbi.nlm.nih.gov/23791887/)
72. Mazurek S. Pyruvate kinase type M2: A key regulator of the metabolic budget system in tumor cells. *Int J Biochem Cell Biol*. 2011; 43(7):969–80. doi: [10.1016/j.biocel.2010.02.005](https://doi.org/10.1016/j.biocel.2010.02.005) WOS:000292362200004. PMID: [20156581](https://pubmed.ncbi.nlm.nih.gov/20156581/)

73. Li Z, Zheng W, Li H, Li C, Gong Z. Synergistic Induction of Potential Warburg Effect in Zebrafish Hepatocellular Carcinoma by Co-Transgenic Expression of Myc and xmrk Oncogenes. *PLoS One*. 2015; 10(7):e0132319. doi: [10.1371/journal.pone.0132319](https://doi.org/10.1371/journal.pone.0132319) PMID: [26147004](https://pubmed.ncbi.nlm.nih.gov/26147004/); PubMed Central PMCID: [PMC4492623](https://pubmed.ncbi.nlm.nih.gov/PMC4492623/).
74. Zhao F, Severson P, Pacheco S, Futscher BW, Klimecki WT. Arsenic exposure induces the Warburg effect in cultured human cells. *Toxicol Appl Pharmacol*. 2013; 271(1):72–7. doi: [10.1016/j.taap.2013.04.020](https://doi.org/10.1016/j.taap.2013.04.020) PMID: [23648393](https://pubmed.ncbi.nlm.nih.gov/23648393/); PubMed Central PMCID: [PMC3714307](https://pubmed.ncbi.nlm.nih.gov/PMC3714307/).